

A switched auxiliary loss for robust training of transformer models for histopathological image segmentation

Saharsh Barve^{1*} and Mustaffa Hussain^{1†}

^{1,2*} Onward Assist, , Bangalore, 560066, Karnataka, India.

*Corresponding author(s). E-mail(s): saharsh@onwardhealth.co;

Contributing authors: mustaffa@onwardhealth.co;

[†]These authors contributed equally to this work.

Abstract

Functional tissue Units (FTUs) are cell population neighborhoods local to a particular organ performing its main function. The FTUs provide crucial information to the pathologist in understanding the disease affecting a particular organ by providing information at the cellular level. In our research, we have developed a model to segment multi-organ FTUs across 5 organs namely: the kidney, large intestine, lung, prostate and spleen by utilizing the 'HuBMAP + HPA - Hacking the Human Body' competition dataset. We propose adding shifted auxiliary loss for training models like the transformers to overcome the diminishing gradient problem which poses a challenge towards optimal training of deep models. Overall, our model achieved a dice score of 0.793 on the public dataset and 0.778 on the private dataset and shows a 1% improvement with the use of the proposed method. The findings also bolster the use of transformers models for dense prediction tasks in the field of medical image analysis. The study assists in understanding the relationships between cell and tissue organization thereby providing a useful medium to look at the impact of cellular functions on human health.

Keywords: semantic segmentation, medical image segmentation, auxiliary loss

Introduction

Convolutional neural networks (CNNs) have been at the forefront of computer vision for tasks like image classification [1, 2], image segmentation [3, 4], and object detection [5, 6]. The applications of such deep learning-based models have proved to be crucial in the recent advancements made in the medical field toward intelligent system-aided predictive analytics [7, 8].

Recently, several researchers have suggested that the transformer encoder models have matched and even outperformed CNNs models in several of the state-of-the-art vision tasks. With the success transformer architectures have achieved, their incorporation into clinical medical practices has tremendous potential in the near future. However, ensuring optimal training of such deep models poses a difficulty because of the diminishing gradients due to infinitesimal losses during the backpropagation. This could affect the model's overall generalizability and robustness, which is crucial, especially in the medical domain.

In this study, we propose the use of shifted auxiliary loss during model training to tackle this problem. We implement the same on 3 transformer models, namely, CoaT [9], Pyramid Vision Transformer-v2 [10] and Segformer [11], in the FTU binary segmentation task. We further implement our approach on common CNN architectures used in the medical domain such as Unet [12] and DeepLabv3+ [13].

Related Work

Dosovitskiy et al. [14] proposed ViT for image classification tasks by using multiple attention heads to create a single-scale low-resolution feature map. To address the limitation posed by single scale output for dense prediction tasks, Wang et al. proposed Pyramid Vision Transformer (PVT) and PVTv2 [10, 15] to generate multiscale feature maps using the hierarchical structure. Segformer created by Enze Xie et al [11] argued to utilize 3x3 convolution using a feed-forward network instead of the conventional positional encoding as suggested by ViT and PVT architectures. Ze Liu et al. [16] provided Swin Transformer architecture, which utilizes window-based self-attention resulting in an improvement in efficiency. Weijian Xu et al. [9] proposed co-scale and conv-attentional mechanisms in their CoaT architecture.

The lightweight characteristic of transformer architecture makes it suitable for working with large medical image datasets. This has led to its application in solving tasks like Brain Tissue Image segmentation [17], myocardial fibrosis tissue detection [18] to name a few. Additionally, new models have also been proposed specifically for medical image analysis, by combining the transformer's encoding capabilities with Unet architecture, such as TransUNet [19], Mix Transformer-Unet [20].

The auxiliary loss was initially proposed in the Inception model [21] with the motivation to overcome the problem posed by diminishing gradients. However, with the introduction of deep architectures such as transformers, Dasol

Han et al. [22] proposed a rebirth of this technique for stable and regularized training of the model. Yechan Yu et al. [23] utilize this to increase the model training by applying the auxiliary loss to each encoder block and helped in improving model accuracy. Yuanfeng Ji et al. [24] utilize this technique in their proposed architecture MC-Transformer to promote proxy-embedded learning.

Experiment

Training

Data

HubMap: Hacking the Human body challenge identifies tissue images comprising five human organs prostate, spleen, lung, kidney and large intestine (Figure 1). Data comes from two different sets of data pools, the Human Protein Atlas (HPA) and the Human BioMolecular Atlas Program (HuBMAP). For training there are 351 images from HPA data of 0.4um in pixel size and 4um in tissue thickness. All HPA images are of size 3000 x 3000 pixels with a tissue area within the image of around 2500 x 2500 pixels. HPA samples are stained with antibodies visualized with 3,3'-diaminobenzidine (DAB) and counter-stained with hematoxylin. The total size of the data is of 9.39GB.

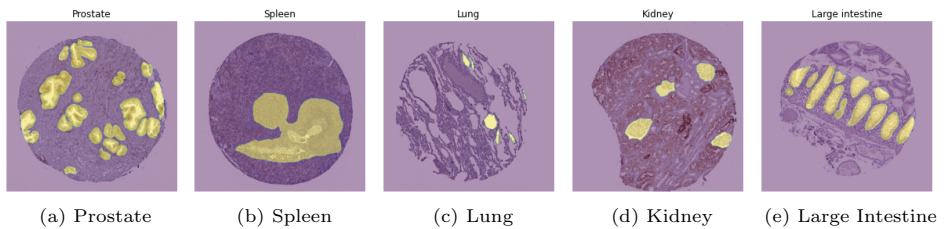


Fig. 1: Train data

Metric

We use the mean Dice coefficient metric for evaluation. The Dice coefficient can be used to compare the pixel-wise agreement between a predicted segmentation and its corresponding ground truth. The formula is given by:

$$\frac{2 * X \cap Y}{X + Y} \quad (1)$$

where X is the predicted set of pixels and Y is the ground truth.

Calculation of Auxiliary Loss

Binary cross entropy loss (BCE) is used to compute the auxiliary loss between the intermediate output at the end of the second block of the encoder against down-sampled mask to the corresponding size. This loss is added along with the main loss and is used for backpropagation. During our training, we shift the auxiliary loss from the second block intermediate output to the first encoder block intermediate output at the end of 60 epochs and further train the model for 60 more epochs.

Training details

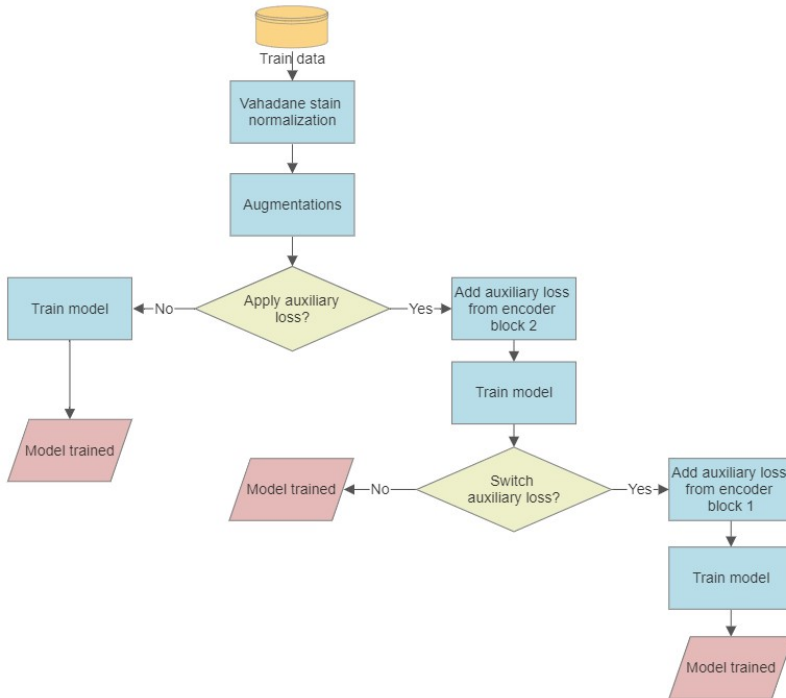


Fig. 2: Model training Framework

For this research, we have utilized Tesla P100-PCIE-16GB GPU with 16GB GDDR6 VRAM for model training and inference. The CPU used is a 1xcore hyper threaded Xeon Processors @2.2Ghz with 15.26GB RAM and disk storage of 155GB.

The data is split into 5 folds using stratified k fold sampling to maintain organ balance between the train and validation dataset. All the HPA images are resized from 3000x3000 to 768x768 for training. We set a batch size of 4 for the training epoch and 8 for the validation epoch as per our hardware

limitation. The models were trained for 120 epochs with a learning rate of $5e-5$ using the ReduceLRonPlateau scheduler.

Figure 2 represents the training framework implemented in our study. The training data is first normalized using the Vahadane stain normalization method [25] to bring uniformity in staining variations present across the HPA and HuBMAP data. The stain target image is a mosaic created using all different staining alterations present in the available data. Medium to heavy augmentations are applied such as spatial level transformations using crop, flip and rotate operations, noise addition, color augmentations like hsv and brightness contrast and finally, elastic transformation and grid distortion are also used. The auxiliary loss is added during the backpropagation from the second encoder block in the first stage and for switch auxiliary loss training after training for 60 epochs the auxiliary loss is switched to the first block of the encoder and trained further for 60 epochs.

Inference

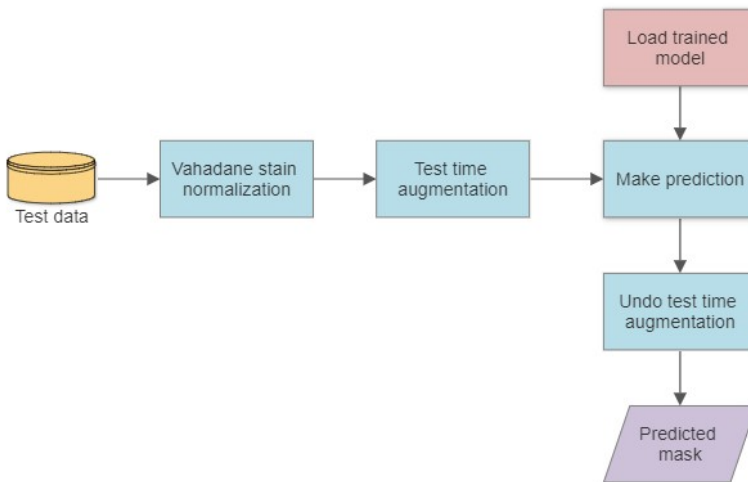


Fig. 3: Inference Framework

Data

HuBMAP images have pixel sizes of $0.5 \mu\text{m}$ for kidney, $0.2290 \mu\text{m}$ for large intestine, $0.7562 \mu\text{m}$ for lung, $0.4945 \mu\text{m}$ for spleen, and $6.263 \mu\text{m}$ for prostate and tissue slice thicknesses of $10 \mu\text{m}$ for kidney, $8 \mu\text{m}$ for large intestine, $4 \mu\text{m}$ for spleen, $5 \mu\text{m}$ for lung, and $5 \mu\text{m}$ for prostate. HuBMAP images were prepared using Periodic acid-Schiff (PAS)/hematoxylin and eosin (H&E)

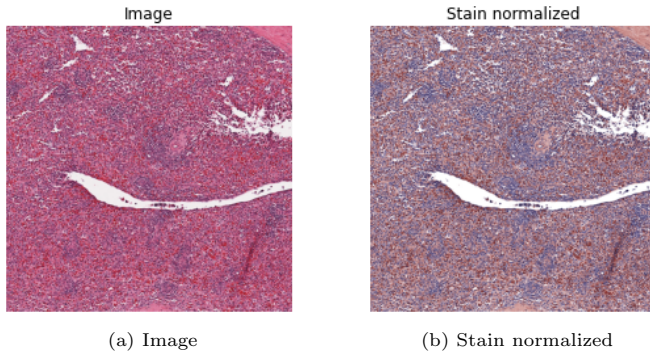


Fig. 4: Sample HuBMAP test image with and without stain normalization

stains. The public tst dataset comprises of HPA and HuBMAP data while the private dataset is made up of only HubMAP data.

Inference details

The inference results have been calculated on a single-fold model. The threshold for generating masks is set as 0.5 for HPA data and 0.4 for HuBMAP data except for lung samples. Furthermore, as the FTU segmentation results for lung are poor as compared to other organs, the threshold is set at 0.15 for HPA lung data and 0.1 for HuBMAP.

During inference, test images are resized to 768 x 768 and then stain normalized using the stain target image (Figure 4), followed by test time augmentation consisting of horizontal and vertical flips. This data is then fed to the trained model and the predicted output from the model based on the organ-specific threshold value is used to generate the final mask.

Results

Figure 5 presents the predicted mask overlay on the sample HuBMAP test image for all of the 9 models trained in our experiments. The models clearly identify the white pulp FTU region of the spleen sample.

Here we try to show the effect of shift auxiliary loss on model generalizability and training. We make use 3 transformer-based models each having a DaFormer decoder [26], CoaT-Daformer, PVTv2-b2-DaFormer and Segformer-Mitb2-DaFormer each of which is trained normally, with single auxiliary loss and with switched auxiliary loss. The results given in Tables 1,3 are as per the submission scores from the competition. We can see a drop of 4% in private dataset scores comprising of only HuBMAP images of varied pixels size and tissue thickness as compared to the public dataset containing HPA and HuBMAP samples. Except for PVTv2 on the public dataset, the rest all the models show a 1% decrease in dice score when trained using a single encoder

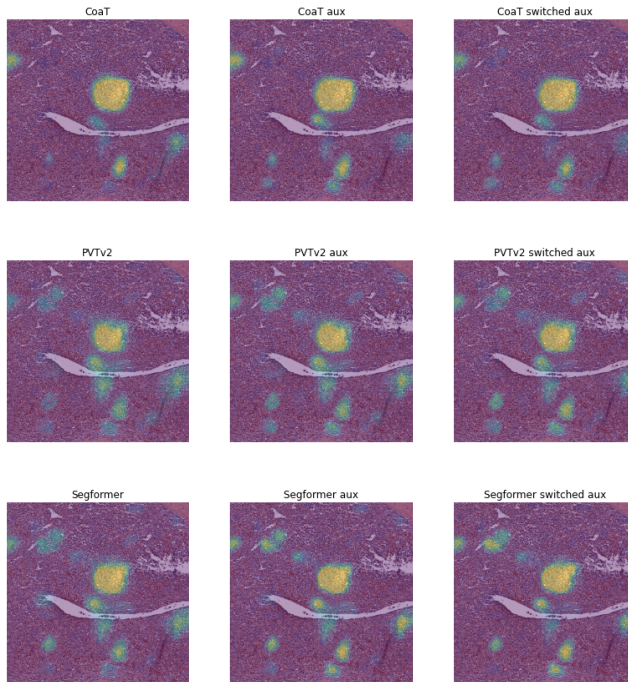


Fig. 5: Results of different models on sample HuBMAP test image of spleen

block auxiliary loss as compared to the normal trained model. However, upon incorporating the switch of auxiliary loss from block 1 to block 2 while training, the models show a 1% improvement than the other two training approaches in both public and private scores.

Table 1: Private HuBMAP dataset (dice score)

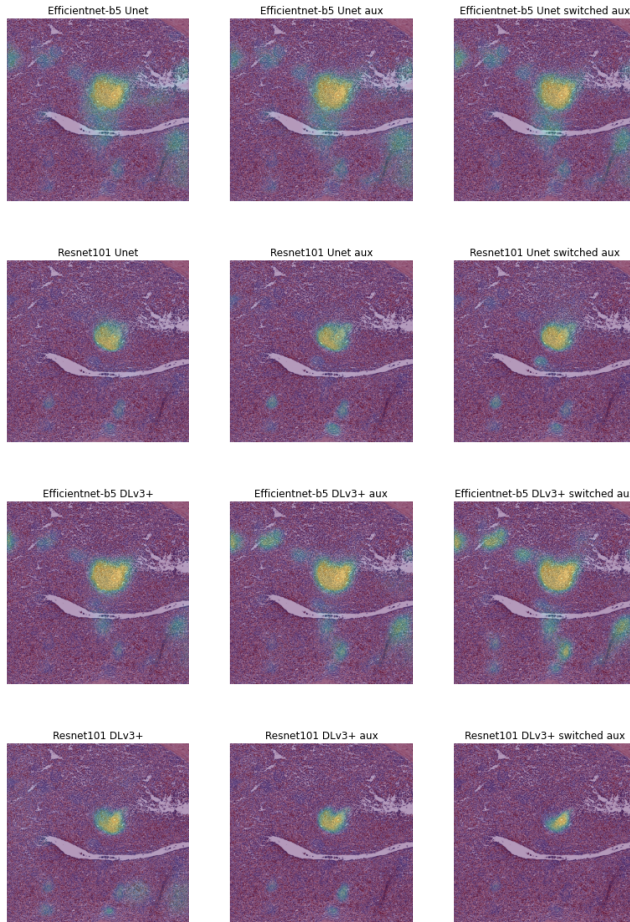
Models	Normal	With Aux Loss	Switched Aux Loss
CoaT	0.76127	0.74223	0.77805
PVTv2	0.69732	0.70284	0.71199
Segformer	0.70640	0.69562	0.72102

Conclusion

While handling strong encoders such as transformers, it is crucial to ensure optimal training of such models wherein there is a negligible gradient from the last layers during back propagation. In this study, we presented a shifted

Table 2: Public HuBMAP + HPA dataset (dice score)

Models	Normal	With Aux Loss	Switched Aux Loss
CoaT	0.78446	0.77024	0.79321
PVTv2	0.74261	0.75728	0.75742
Segformer	0.76105	0.75931	0.76628

**Fig. 6:** Results of CNN models on sample HuBMAP test image of spleen

auxiliary loss to make the problem more difficult for the model thus ensuring larger loss and inturn more gradient in the back propagation stage. This approach was implemented for training 3 deep transformer-based models for the task of image segmentation. We used the HuBMAP + HPA: Hacking the

Table 3: Public HuBMAP + HPA dataset (dice score) CNN models

Models	Normal	With Aux Loss	Switched Aux Loss
Enet-b5 Unet	0.77197	0.76929	0.75352
Resnet101 Unet	0.69737	0.70302	0.67994
Enet-b5 DLv3+	0.75404	0.75438	0.75921
Resnet101 DLv3+	0.60265	0.65143	0.66397

Human Body competition dataset to demonstrate this approach's effectiveness and support the utilization of lightweight transformer models for dense prediction tasks in the medical domain. The results showed that the switched auxiliary loss approach provided an improvement of 1% as compared to other methods across all the different models implemented. The CoaT model performed the best in the task with a score of 0.778 followed by Segformer and PVTv2. The findings from our study can be implemented to improve model training and robustness.

Appendix

We also conducted experiments with effects of auxiliary loss in training of models based on convolution n networks. Figure 6 shows the results obtained using CNN-based models. It can be seen from 3 that auxiliary loss brings in improvement as compared to the normal approach, though switched auxiliary loss failed to boost the training metrics. Further studies can focus on investigating the application of switched auxiliary loss for convolutional neural network-based architectures.

References

- [1] Maggiori, E., Tarabalka, Y., Charpiat, G., Alliez, P.: Fully convolutional neural networks for remote sensing image classification. In: 2016 IEEE International Geoscience and Remote Sensing Symposium (IGARSS), pp. 5071–5074 (2016). <https://doi.org/10.1109/IGARSS.2016.7730322>
- [2] Rawat, W., Wang, Z.: Deep Convolutional Neural Networks for Image Classification: A Comprehensive Review. *Neural Computation* **29**(9), 2352–2449 (2017) https://direct.mit.edu/neco/article-pdf/29/9/2352/1017965/neco_a_00990.pdf. https://doi.org/10.1162/neco_a.00990
- [3] Guo, Y., Liu, Y., Georgiou, T., Lew, M.S.: A review of semantic segmentation using deep neural networks. *International Journal of Multimedia Information Retrieval* **7**, 87–93 (2017)
- [4] Long, J., Shelhamer, E., Darrell, T.: Fully convolutional networks for semantic segmentation. *CoRR* **abs/1411.4038** (2014) [1411.4038](https://arxiv.org/abs/1411.4038)

- [5] Lin, T., Dollár, P., Girshick, R.B., He, K., Hariharan, B., Belongie, S.J.: Feature pyramid networks for object detection. CoRR **abs/1612.03144** (2016) [1612.03144](#)
- [6] Zhu, Y., Zhao, C., Guo, H., Wang, J., Zhao, X., Lu, H.: Attention couplenet: Fully convolutional attention coupling network for object detection. IEEE Transactions on Image Processing **28**(1), 113–126 (2019). <https://doi.org/10.1109/TIP.2018.2865280>
- [7] Kayalibay, B., Jensen, G., van der Smagt, P.: Cnn-based segmentation of medical imaging data. CoRR **abs/1701.03056** (2017) [1701.03056](#)
- [8] Zhang, H., Ma, T.: Acne detection by ensemble neural networks. Sensors **22**(18) (2022). <https://doi.org/10.3390/s22186828>
- [9] Xu, W., Xu, Y., Chang, T.A., Tu, Z.: Co-scale conv-attentional image transformers. CoRR **abs/2104.06399** (2021) [2104.06399](#)
- [10] Wang, W., Xie, E., Li, X., Fan, D., Song, K., Liang, D., Lu, T., Luo, P., Shao, L.: Pvtv2: Improved baselines with pyramid vision transformer. CoRR **abs/2106.13797** (2021) [2106.13797](#)
- [11] Xie, E., Wang, W., Yu, Z., Anandkumar, A., Alvarez, J.M., Luo, P.: Segformer: Simple and efficient design for semantic segmentation with transformers. CoRR **abs/2105.15203** (2021) [2105.15203](#)
- [12] Ronneberger, O., Fischer, P., Brox, T.: U-net: Convolutional networks for biomedical image segmentation. CoRR **abs/1505.04597** (2015) [1505.04597](#)
- [13] Chen, L., Zhu, Y., Papandreou, G., Schroff, F., Adam, H.: Encoder-decoder with atrous separable convolution for semantic image segmentation. CoRR **abs/1802.02611** (2018) [1802.02611](#)
- [14] Dosovitskiy, A., Beyer, L., Kolesnikov, A., Weissenborn, D., Zhai, X., Unterthiner, T., Dehghani, M., Minderer, M., Heigold, G., Gelly, S., Uszkoreit, J., Houlsby, N.: An image is worth 16x16 words: Transformers for image recognition at scale. CoRR **abs/2010.11929** (2020) [2010.11929](#)
- [15] Wang, W., Xie, E., Li, X., Fan, D., Song, K., Liang, D., Lu, T., Luo, P., Shao, L.: Pyramid vision transformer: A versatile backbone for dense prediction without convolutions. CoRR **abs/2102.12122** (2021) [2102.12122](#)
- [16] Liu, Z., Lin, Y., Cao, Y., Hu, H., Wei, Y., Zhang, Z., Lin, S., Guo, B.: Swin transformer: Hierarchical vision transformer using shifted windows. CoRR **abs/2103.14030** (2021) [2103.14030](#)

- [17] Zhang, J., Zhao, L., Zeng, J., Qin, P.: Sf-segformer: Stepped-fusion segmentation transformer for brain tissue image via inter-group correlation and enhanced multi-layer perceptron. In: Yang, G., Aviles-Rivero, A., Roberts, M., Schönlieb, C.-B. (eds.) *Medical Image Understanding and Analysis*, pp. 508–518. Springer, Cham (2022)
- [18] Ding, Y., Xie, W., Liao, Z., Wong, K.K.L.: De-mri myocardial fibrosis segmentation and classification model based on multi-scale self-supervision and transformer. *Computer Methods and Programs in Biomedicine*, 107049 (2022). <https://doi.org/10.1016/j.cmpb.2022.107049>
- [19] Chen, J., Lu, Y., Yu, Q., Luo, X., Adeli, E., Wang, Y., Lu, L., Yuille, A.L., Zhou, Y.: Transunet: Transformers make strong encoders for medical image segmentation. *CoRR* **abs/2102.04306** (2021) [2102.04306](https://arxiv.org/abs/2102.04306)
- [20] Wang, H., Xie, S., Lin, L., Iwamoto, Y., Han, X.-H., Chen, Y.-W., Tong, R.: Mixed transformer u-net for medical image segmentation, pp. 2390–2394 (2022). <https://doi.org/10.1109/ICASSP43922.2022.9746172>
- [21] Szegedy, C., Liu, W., Jia, Y., Sermanet, P., Reed, S.E., Anguelov, D., Erhan, D., Vanhoucke, V., Rabinovich, A.: Going deeper with convolutions. *CoRR* **abs/1409.4842** (2014) [1409.4842](https://arxiv.org/abs/1409.4842)
- [22] Han, D., Yoo, J., Oh, D.: Seethroughnet: Resurrection of auxiliary loss by preserving class probability information. In: *2022 IEEE/CVF Conference on Computer Vision and Pattern Recognition (CVPR)*, pp. 4453–4462 (2022). <https://doi.org/10.1109/CVPR52688.2022.00442>
- [23] Yu, Y., Park, D., Kim, H.K.: Auxiliary Loss of Transformer with Residual Connection for End-to-End Speaker Diarization. *arXiv* (2021). <https://doi.org/10.48550/ARXIV.2110.07116>. <https://arxiv.org/abs/2110.07116>
- [24] Ji, Y., Zhang, R., Wang, H., Li, Z., Wu, L., Zhang, S., Luo, P.: Multi-compound transformer for accurate biomedical image segmentation. In: de Bruijne, M., Cattin, P.C., Cotin, S., Padoy, N., Speidel, S., Zheng, Y., Essert, C. (eds.) *Medical Image Computing and Computer Assisted Intervention – MICCAI 2021*, pp. 326–336. Springer, Cham (2021)
- [25] Vahadane, A., Peng, T., Albarqouni, S., Baust, M., Steiger, K., Schlitter, A.M., Sethi, A., Esposito, I., Navab, N.: Structure-preserved color normalization for histological images. In: *2015 IEEE 12th International Symposium on Biomedical Imaging (ISBI)*, pp. 1012–1015 (2015). <https://doi.org/10.1109/ISBI.2015.7164042>
- [26] Hoyer, L., Dai, D., Gool, L.V.: Daformer: Improving network architectures and training strategies for domain-adaptive semantic segmentation. *CoRR* **abs/2111.14887** (2021) [2111.14887](https://arxiv.org/abs/2111.14887)